

Article

Spatiotemporal Distribution Characteristics of Copepods in the Water Masses of the Northeastern East China Sea

Sang Su Shin ^{1,†}, Seo Yeol Choi ^{2,†} , Min Ho Seo ¹, Seok Ju Lee ³, Ho Young Soh ^{2,*} and Seok Hyun Youn ^{4,*}

¹ Marine Ecology Research Center, Yeosu 59697, Korea; shinsangsu3@gmail.com (S.S.S.); copepod79@gmail.com (M.H.S.)

² Department of Marine Integrated Science, Chonnam National University, Yeosu 59626, Korea; seoyeol84@gmail.com

³ Marine Biological Resource Center, Yeosu 59697, Korea; sjlee840425@gmail.com

⁴ Oceanic Climate and Ecology Research Division, National Institute of Fisheries Science, Busan 46083, Korea

* Correspondence: hysoh@chonnam.ac.kr (H.Y.S.); younsh@korea.kr (S.H.Y.)

† These authors contributed equally to this work.

Abstract: To understand the effects of variable water masses in the northeastern East China Sea (Korea South Sea), planktonic copepods were seasonally sampled. Out of a total of 106 copepod species, 85 were oceanic warm-water species, and the number of species varied in summer, autumn, spring, and winter. The study area was divided into two or three regions according to the degree of influence of the water masses. *Canthocalanus pauper*, *Clausocalanus furcatus*, *Oithona plumifera*, *Oncaea venella*, *Oncaea venusta*, and *Paracalanus aculeatus* showed a positive correlation with water temperature and salinity and were indicator species of warm currents. *Calanus sinicus*, known as an indicator species of the Yellow Sea Bottom Cold Water, showed a high abundance and occurrence ratio in the western sea of the study area from spring to autumn. Moreover, *Acartia pacifica* indicated the extension of coastal waters to offshore areas. Several oceanic warm-water species (*A. danae*, *Centropages gracilis*, *Labidocera acuta*, *Rhincalanus nasutus*, and *Temoropia mayumbaensis*) were considered indicator species of the Taiwan Warm Current. Our results suggest that the spatiotemporal distribution patterns of indicator species are partly explained by different water masses.

Keywords: East China Sea; warm currents; copepods; indicators; spatiotemporal distribution



Citation: Shin, S.S.; Choi, S.Y.; Seo, M.H.; Lee, S.J.; Soh, H.Y.; Youn, S.H. Spatiotemporal Distribution Characteristics of Copepods in the Water Masses of the Northeastern East China Sea. *J. Mar. Sci. Eng.* **2022**, *10*, 754. <https://doi.org/10.3390/jmse10060754>

Academic Editor: Marco Uttieri

Received: 29 April 2022

Accepted: 27 May 2022

Published: 30 May 2022

Publisher's Note: MDPI stays neutral with regard to jurisdictional claims in published maps and institutional affiliations.



Copyright: © 2022 by the authors. Licensee MDPI, Basel, Switzerland. This article is an open access article distributed under the terms and conditions of the Creative Commons Attribution (CC BY) license (<https://creativecommons.org/licenses/by/4.0/>).

1. Introduction

In the marine ecosystem, zooplankton, particularly copepods, occupy an important intermediate position, transmitting energy to upper trophic levels as they feed on phytoplankton, grow, and are consumed by predators [1]. Moreover, copepods have limited locomotion ability to move against the flow of water masses and are sensitive to changes within them. They have been used as indicators of changes in water masses and ocean currents [2–6]. In particular, *Clausocalanus furcatus*, *Oithona plumifera*, *Paracalanus aculeatus*, and *Oncaea venusta* have been used as indicator species for the inflow of the Tsushima Warm Current [5,7–9], and *Calanus sinicus* has been used as an indicator species for the inflow of the Yellow Sea Bottom Cold Water (YSBCW) to the East China Sea [10,11]. Furthermore, the coastal species *Acartia omorii* and *Paracalanus parvus* s. l. were used as indicator species for the expansion of coastal waters into the open sea [12,13].

Changes in water masses generally cause a seasonal succession of zooplankton, fluctuations in abundance, and the distribution of diverse community structures or species [2,14]. Therefore, zooplankton have generally been used as indicators of water masses and ocean currents [4,5]. Changes in physical environmental factors, such as the temperature and salinity of marine ecosystems, can lead to rapid changes in the species richness and quantitative characteristics of zooplankton [4,5]. Water masses or currents vary in their extent of expansion according to the season, and when different water masses meet each other,

they mix or form a front. The seasonal influence of water masses acts as a major factor in changing the distribution pattern and community structure of zooplankton [15,16]. In the northeastern East China Sea (nECS), zooplankton are expected to distinctly define their habitat characteristics in response to a variety of physical environmental variables. Various studies on the characteristics of water masses that affect the distribution of copepods and chaetognaths [16,17], the seasonal vertical distribution characteristics of copepods [18], and the environmental factors affecting neustonic zooplankton in summer [19] have been conducted in a part of the nECS. However, as these studies were conducted in a limited area or only in one season, there is a limited understanding of the effects of various water masses or currents in the nECS. Therefore, the purpose of this study was to understand the effects of these seasonal water masses on changes in the planktonic copepod community structure and to clarify the relationship between environmental factors and indicator species that could explain the effect of water masses or currents in the entire nECS.

2. Materials and Methods

2.1. Study Sites and Environmental Factors

The study area is a site with a widely developed continental shelf at a depth of 200 m or less, and is connected to the Yellow Sea, East China Sea, and East Sea (Sea of Japan). There are also various water masses or warm currents. The Tsushima Warm Current (TWC), characterized by high temperature and salinity, originates from the Kuroshio Water (KW) and flows into the East Sea from the East China Sea. The YSBCW, with a low water temperature, originates from the Yellow Sea in winter, moves south in summer, and affects the bottom layer. Moreover, in the summer, the Changjiang diluted water (CDW), which comprises a mixture of surface water and fresh water from the Changjiang River, has a low salinity effect on the study area. In addition, the Taiwan Warm Current (TAWC) and Chinese coastal waters affect the study area [20–22].

Field surveys were conducted seasonally in the nECS (Figure 1, Table 1). Water temperature and salinity were vertically measured using a calibrated SBE 9/11 plus CTD instrument (Sea-Bird Electronics, Bellevue, WA, USA). Seawater was sampled for estimating the chlorophyll-*a* concentration (Chl-*a*) using Niskin water samplers that were attached to the same equipment according to water depths of 0, 10, 20, 30, 50, 75, 100, and 125 m.

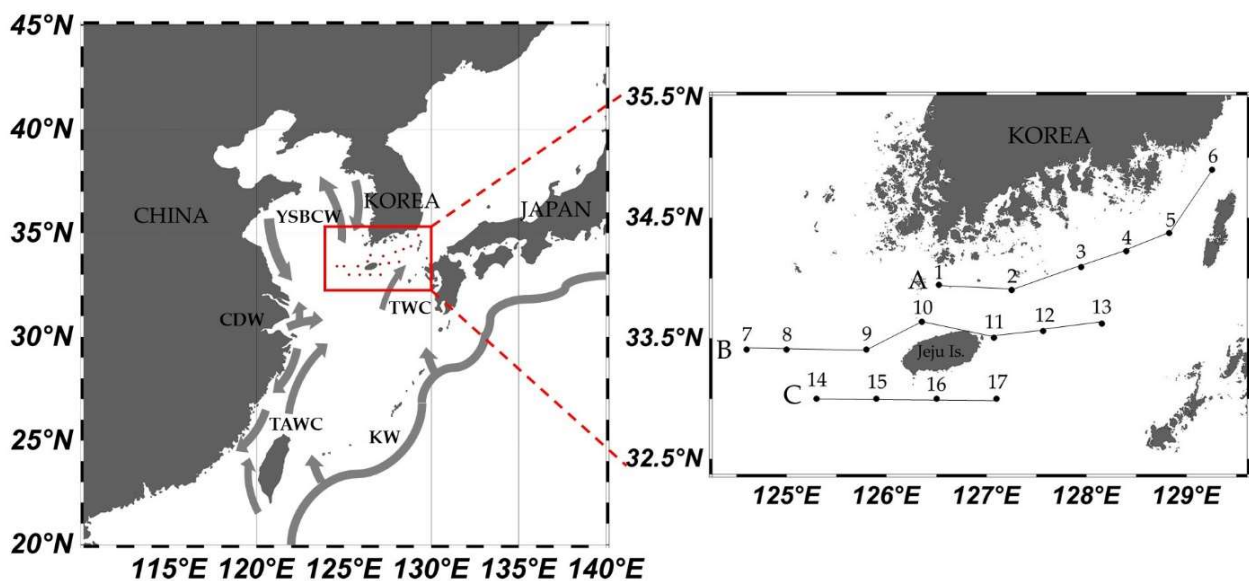


Figure 1. Map of the study sites. Abbreviations: CDW: Changjiang diluted water; Jeju Is.: Jeju Island; TWC: Tsushima Warm Current; TAWC: Taiwan Warm Current water; YSBCW: Yellow Sea bottom cold water; and KW: Kuroshio water.

Table 1. Geographic coordinates of the study sites in the Korea South Sea.

Station	Latitude	Longitude	Bottom Depth (m)
1	33.9	126.5	52
2	33.9	127.3	78
3	34.1	127.9	82
4	34.2	128.4	85
5	34.4	128.8	102
6	34.9	129.3	127
7	33.4	124.6	75
8	33.4	125.0	125
9	33.4	125.8	92
10	33.6	126.4	140
11	33.5	127.1	128
12	33.6	127.6	102
13	33.6	128.2	119
14	33.0	125.3	85
15	33.0	125.9	102
16	33.0	126.5	107
17	33.0	127.1	105

To measure Chl-*a* by size (>20 μm , 3–20 μm , <3 μm), a 20-micrometer membrane filter (Polycarbonate Track Etched, 47 mm; GVS, Sanford, ME, USA), 3-micrometer PC membrane filters (polycarbonate membrane filter, 47 mm; Whatman, Florham Park, NJ, USA), and a 0.45-micrometer membrane filter (polycarbonate membrane filter, 47 mm; Advantec, Tokyo, Japan) were used for sequential filtration by size through a filter holder. Next, the membrane filter was placed in a conical tube (15 mL), wrapped in aluminum foil, and stored at $-80\text{ }^{\circ}\text{C}$. All filters were then transferred to frozen storage in our laboratory. Chl-*a* was extracted after solvation in 90% acetone, and they were settled in a dark and cool chamber for 24 h. To filter out particles and extract them from the filter paper, a syringe filter (0.45 μm , polytetrafluoroethylene; Advantec, Florham Park, NJ, USA) was used for filtration and the absorbance was measured using a fluorometer (10-Au; Tuner Designs, San Jose, CA, USA) calibrated with a Chl-*a* standard (Sigma-Aldrich, Darmstadt, Germany). Next, Chl-*a* concentration was calculated from the absorbance measurement using the UNESCO formula [23].

2.2. Zooplankton Sampling

The zooplankton were vertically towed from the bottom 3 m to the surface layer of each station using a conical zooplankton net (mouth size 60 cm, mesh size 200 μm) in February (winter), April (spring), August (summer), and October (autumn) 2018 (Figure 1). The samples were immediately fixed on board at a final concentration of 5–10% with neutralized formaldehyde seawater. A flow meter (model 438115; Hydro-Bios co., Altenholz, Germany) was attached to the inlet of the net to calculate the amount of filtered seawater that passed through the net. Next, the samples were divided into 1:2–1:512 to determine the species composition and abundance of zooplankton using a Folsom-type divider until the final abundance reached approximately 300 or more. Species identification was performed under an optical microscope (SMZ645; Nikon, Tokyo, Japan). When more detailed observation was needed for species identification, the appendages with characteristic features of the species were dissected and observed on a glass slide with an optical microscope (ECLIPSE 80i; Nikon). Next, the zooplankton sample measurements were converted to the number of individuals per unit volume (ind m^{-3}).

2.3. Data Analysis

To understand the characteristics of the water masses in the study area, a T-S diagram (temperature–salinity) was constructed using the water temperature and salinity data (Figure 2). The water masses were classified according to their physical properties as

follows: the TWC has a water temperature of 15 °C or higher and salinity of 31–34.5 psu [24]; the YBCW has a water temperature of 13.2 °C or lower and salinity of 32.6–33.7 psu or lower [25]; and the CDW has a water temperature of 23 °C or higher and salinity of 31 psu or lower [26]. After setting three north-to-south lines (A, B, and C lines), each vertical sectional diagram was drawn using Ocean Data View 5.5.1 software to determine the distribution of the water masses that were affected by the water depth of the study area (Figures 2 and 3). A horizontal cross-sectional diagram for Chl-*a* was also drawn (see Supplementary Material Figure S1).

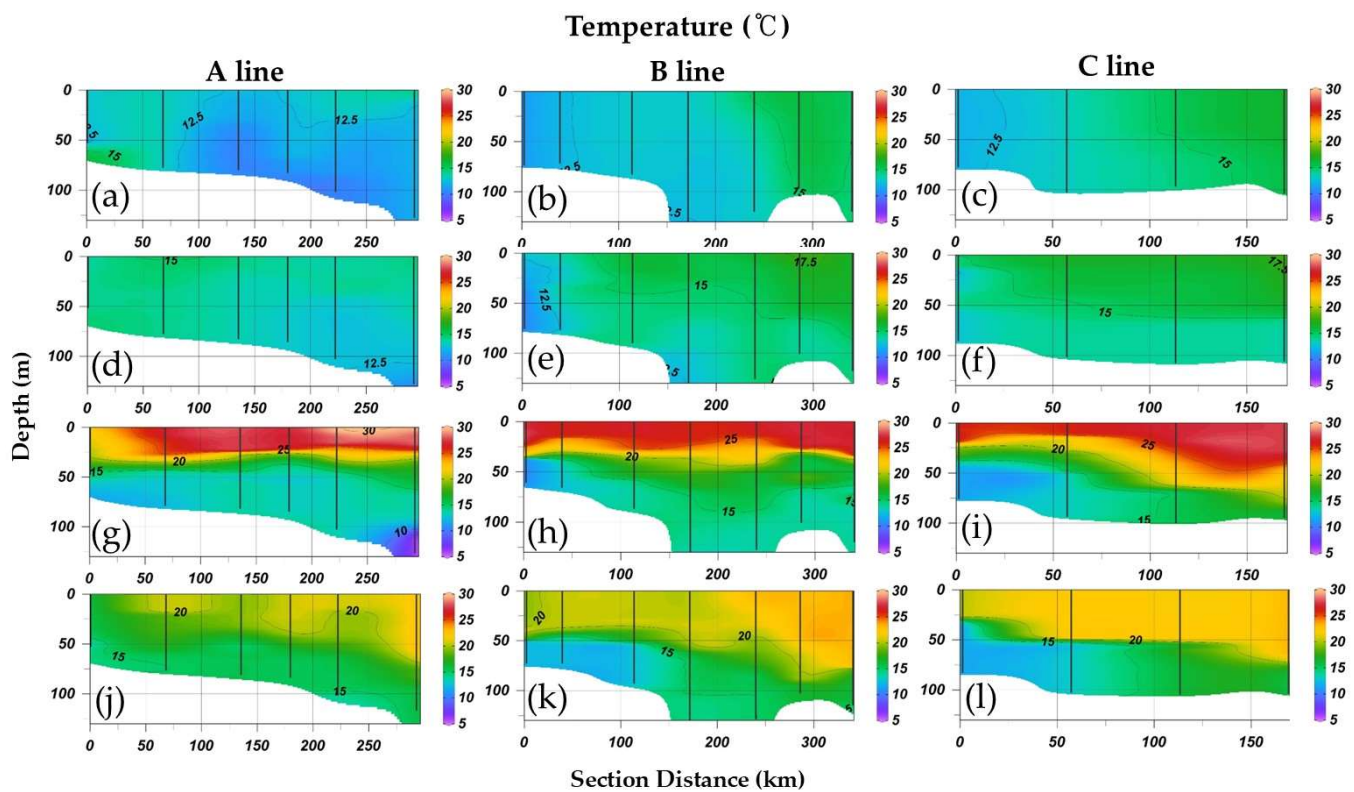


Figure 2. Vertical distribution of water temperature (°C) in (a–c) February, (d–f) April, (g–i) August, and (j–l) October 2018. Lines A, B, and C represent north-to-south sampling lines in the study area.

A cluster analysis was performed to compare the similarities between stations based on copepod abundance identified to the species level using PRIMER software (version 6.1.6). After the abundances were converted to Log (x + 1) to reduce the bias in the distribution of the data due to the variation in the abundances, the Bray–Curtis similarity index was calculated. Based on this index, a hierarchical cluster analysis was performed using the unweighted pair group method with arithmetic mean (UPGMA) and compared to the non-metric multidimensional scaling (nMDS) arrangement method. Next, the similarity index for grouping the stations was divided into 50% in February, 55% in April, 53% in August, and 60% in October, and was further subdivided into 55% and 60% in August and October, respectively. The similarity-percentages procedure (SIMPER) analysis was completed to select the major species that affected each classified cluster [27]. In addition, a canonical correspondence analysis (CCA) was conducted using Canonical Community Ordination (CANOCO) software (version 4.5) to examine the relationship between the major species that contributed to the group classification seasonally and the environmental factors (water temperature, salinity, and fractional Chl-*a* by size) [28]. Additionally, a Pearson correlation analysis in the statistical package SPSS (version 12.0) was used to determine the correlation between these major species and the environmental factors (water temperature, salinity, and fractional Chl-*a* by size) of the study area ($p < 0.01$; $p < 0.05$). Data normality was checked

before analysis. When data were not normally distributed, a $\log(x + 1)$ transformation was applied for data normality.

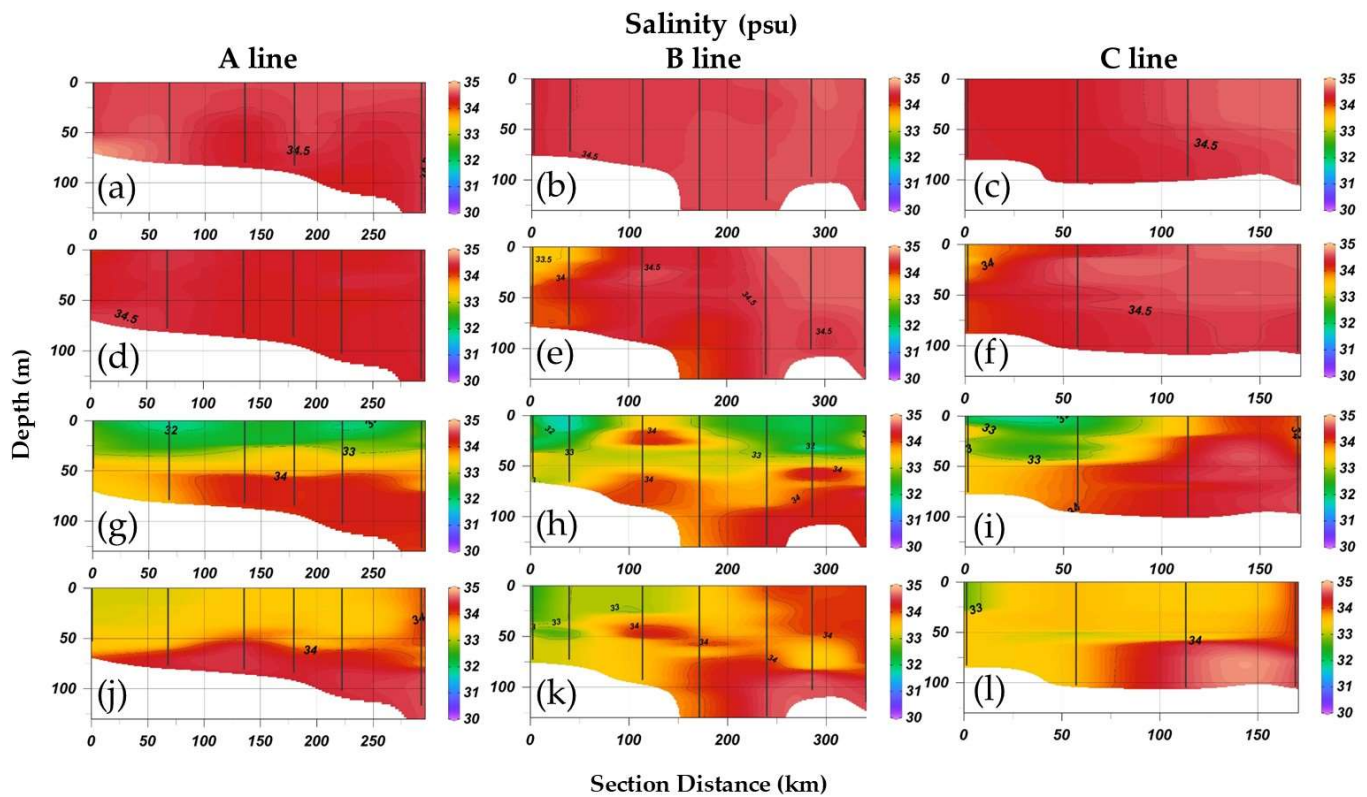


Figure 3. Vertical distribution of salinity (psu) in (a–c) February, (d–f) April, (g–i) August, and (j–l) October 2018. Lines A, B, and C represent north-to-south sampling lines in the study area.

3. Results

3.1. Environmental Factors (Water Temperature, Salinity, and Chl-a Concentration)

In February, the water temperature and salinity were in the range of 10.2–16.4 °C and 34.27–34.67 psu, respectively (Figures 2 and 3a–c). The TWC was observed at stations 12 and 13 on the eastern side of Line B and stations 16 and 17 on the eastern side of Line C, and there was a difference of approximately 5 °C in the water temperature when compared to the other stations. Moreover, there was no difference between the surface and bottom layers at the observatory in February (Figures 2 and 3a–c).

In April, the water temperature and salinity were in the range of 10.4–17.6 °C and 33.48–34.67 psu, respectively (Figures 2 and 3d–f). The TWC was observed at stations 9–13 on the eastern side of Line B, and at stations 14 and 15 on the eastern side of Line C. The YSBCW was observed at station 7 on the western side of Line B and station 14 on the western side of Line C, and was located approximately 25 m from the surface (Figures 2 and 3d–f).

In August, the water temperature and salinity were in the range of 6.1–28.3 °C and 31.73–34.59 psu, respectively (Figures 2 and 3g–i). The TWC was observed at all the stations. The YSBCW was observed at stations 7–9 on the western side of Line B and at stations 14 and 15 on the western side of Line C, and it was located at water depths of approximately 50 m or deeper (Figures 2 and 3g–i).

In October, the water temperature and salinity were in the range of 11.7–23.5 °C and 32.42–34.64 psu, respectively (Figures 2 and 3j–l). The TWC was observed at all the stations, as was the case in August. The YSBCW was observed at stations 7–9 west of Line B and stations 14 and 15 of Line C, and was located at water depths of approximately 50 m or deeper (Figures 2 and 3j–l).

The Chl-*a* concentration was high in April and October, whereas it was low in February and August. The stations that were adjacent to the coast had higher Chl-*a* concentrations than those in the open sea (Table 2; see Supplementary Material Figure S1).

Table 2. Range of total chlorophyll-*a* concentrations ($\mu\text{g/L}$), microplankton ($>20\ \mu\text{m}$), nanoplankton ($3\text{--}20\ \mu\text{m}$), and pico-plankton ($<3\ \mu\text{m}$) in the Korea South Sea.

Months	Total		Micro		Nano		Pico	
	Min	Max	Min	Max	Min	Max	Min	Max
2	0.01 (St. 3)	1.64 (St. 17)	0 (St. 2, 3, 5, 10, 13)	0.88 (St. 17)	no data	no data	no data	no data
4	0.52 (St. 15)	4.65 (St. 6)	0.05 (St. 10)	1.17 (St. 13)	0 (except St. 16)	0.01 (St. 16)	0.19 (St. 9)	1.95 (St. 6)
8	0.15 (St. 4)	0.81 (St. 1)	0.02 (St. 13)	0.23 (St. 17)	0.04 (St. 12, 16)	0.11 (St. 7)	0.15 (St. 6)	0.44 (St. 1)
10	0.61 (St. 17)	4.12 (St. 4)	0.02 (St. 1)	1.91 (St. 4)	0.08 (St. 17)	0.25 (St. 1, 8)	0.25 (St. 16)	0.81 (St. 8)

In February, the total Chl-*a* concentration was in the range of 0.01–1.64 $\mu\text{g/L}$, with the highest value at station 17 and the lowest at station 3. The $>20\text{-micrometer}$ Chl-*a* concentration was in the range of 0–0.88 $\mu\text{g/L}$, with the highest value at station 17, and concentrations of $<0.3\ \mu\text{g/L}$ Chl-*a* were observed at the other stations (Table 2; see Supplementary Material Figure S1).

In April, the range of the total Chl-*a* concentration was 0.52–4.65 $\mu\text{g/L}$, with the highest value at station 6 at 4.65 $\mu\text{g/L}$ and the lowest at 0.52 $\mu\text{g/L}$ at station 15 (Table 2; see Supplementary Material Figure S1). The $>20\text{-micrometer}$ Chl-*a* concentration was in the range of 0.05–1.17 $\mu\text{g/L}$, with the highest value at station 13 and the lowest at station 10. The Chl-*a* concentration measuring between 3 μm and 20 μm ranged from 0 to 0.01 $\mu\text{g/L}$ and was hardly observed at almost all stations. The $<3\text{-micrometer}$ Chl-*a* concentration was in the range of 0.28–1.95 $\mu\text{g/L}$, with the highest value at station 6 and the lowest at station 15. The total Chl-*a* concentration was observed to be high close to the coast of the eastern sea area and further from Jeju Island. The $>20\text{-micrometer}$ Chl-*a* was observed to be at a relatively high concentration in the seas near the east of Jeju Island, whereas a relatively high concentration of $<3\ \mu\text{m}$ Chl-*a* was observed at the stations that were adjacent to the east coast of the study area (Table 2; see Supplementary Material Figure S1).

In August, the total Chl-*a* ranged from 0.15 to 0.81 $\mu\text{g/L}$, with the highest value at station 1 and the lowest values at stations 3 and 4. The $>20\text{-micrometer}$ Chl-*a* was in the range of 0.02–0.23 $\mu\text{g/L}$, with the highest value at station 17 and the lowest at station 13. The Chl-*a* measuring between 3 μm and 20 μm was in the range of 0.04–0.11 $\mu\text{g/L}$, with the highest values at stations 1 and 7, and the lowest at station 16. The Chl-*a* measuring $<3\ \mu\text{m}$ or less ranged from 0.15 to 0.38 $\mu\text{g/L}$, with the highest value at station 7 and the lowest at station 6. This was similar to the $<3\text{micrometer}$ Chl-*a* levels in February and was observed to be $<1\ \mu\text{g/L}$ (Table 2; see Supplementary Material Figure S1).

In October, the total Chl-*a* ranged from 0.61–4.12 $\mu\text{g/L}$, with the highest value at station 4, and the lowest at station 17 (Table 2; see Supplementary Material Figure S1). The $>20\text{micrometer}$ Chl-*a* concentrations were in the range of 0.02–1.91 $\mu\text{g/L}$, with the highest value at station 4, and the lowest at station 1. The Chl-*a* concentration measuring between 3 μm and 20 μm was in the range of 0.08–0.25 $\mu\text{g/L}$, with the highest value at station 1, and the lowest at station 12. The Chl-*a* concentration measuring 3 μm or less ranged from 0.25 to 0.81 $\mu\text{g/L}$, with the highest value at station 8, and the lowest at station 16. As in April, the Chl-*a* concentration was relatively high close to the east coast and further from Jeju Island. The Chl-*a* measuring 20 μm or more were observed to be at a relatively high concentration at the stations that were adjacent to the east coast of the study area, whereas at the other stations, Chl-*a* occurred at a concentration of less than 1 $\mu\text{g/L}$ (Table 2; see Supplementary Material Figure S1).

3.2. Spatiotemporal Distribution of the Copepods

Supplementary Material Table S1 shows the species list and relative occurrence ratio of copepods in the study area. In total, 106 species of planktonic copepods were observed. The numbers of warm-water oceanic species observed were 39 of the 54 species in February, 34 of the 48 species in April, 66 of the 75 species in August, and 56 of the 66 species in October. The major species that were recorded were as follows: *Calanus sinicus*, *Ctenocalanus vanus*, *Oithona longispina*, *Oithona plumifera*, *P. aculeatus*, *P. parvus* s. l., *Scolecithricella longispinosa*, and *S. nicobarica* in the winter; *Ctenocalanus vanus*, *Ditrichocorycaeus affinis*, *Oithona longispina*, *Oithona similis*, *Paracalanus parvus* s. l. in the spring; *A. pacifica*, *Calanus sinicus*, *Canthocalanus pauper*, *Clausocalanus furcatus*, *D. affinis*, *Oncaea venella*, *Oncaea venusta*, *Oithona atlantica*, *Paracalanus parvus* s. l., *Paracalanus aculeatus*, and *Undinula vulgaris* in the summer; and *A. pacifica*, *Clausocalanus furcatus*, *Canthocalanus pauper*, *Clausocalanus minor*, *D. affinis*, *Farranula gibbula*, *Oithona atlantica*, *Oithona plumifera*, *Oncaea venella*, *Oncaea venusta*, *Paracalanus aculeatus*, and *Paracalanus parvus* s. l. in the autumn.

The abundance of the copepods was in the range of 87–800 ind m⁻³ in February, with the lowest value at station 8 and the highest at station 17. In April, it was in the range of 300–3270 ind m⁻³, with the lowest value at station 13 and the highest at station 7. In August, it was in the range of 258–1647 ind m⁻³, with the lowest value at station 11 and the highest at station 10. In October, it was in the range of 270–1080 ind m⁻³, with the lowest value at station 16 and the highest at station 12 (Figure 4).

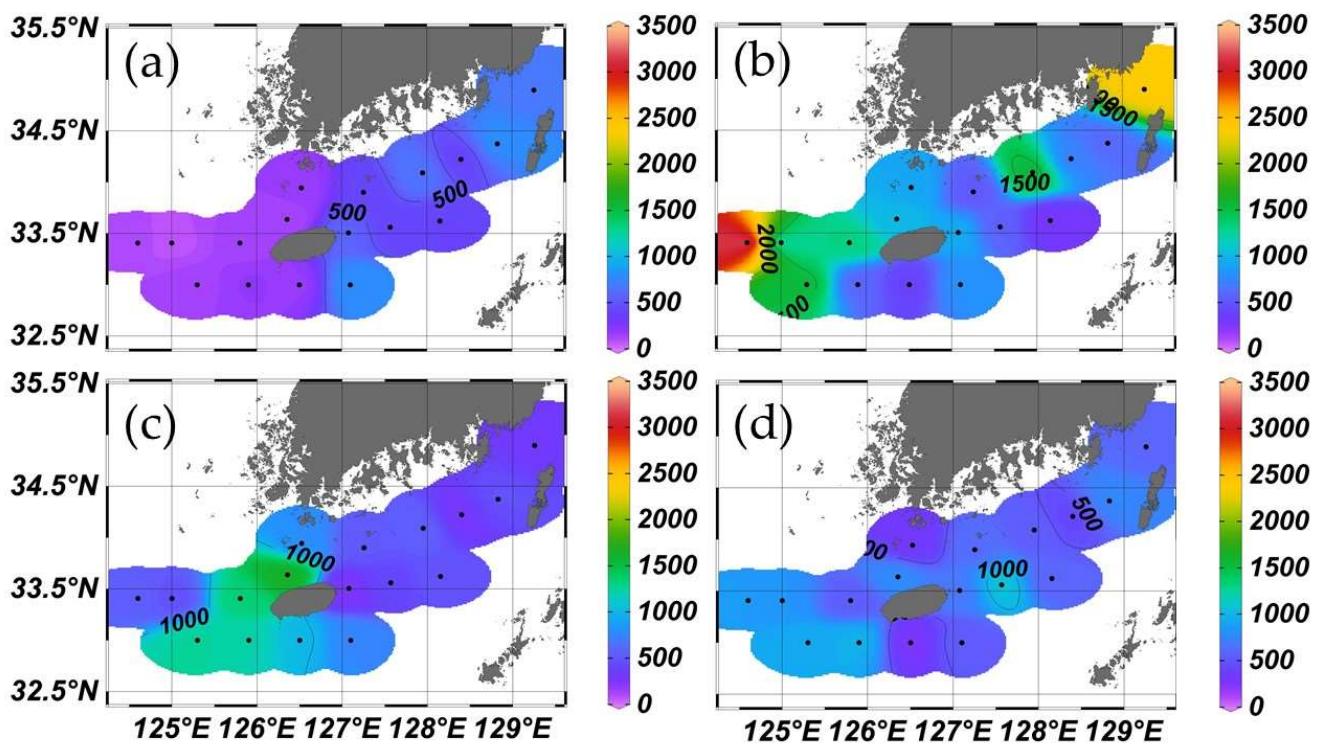


Figure 4. Distribution of copepod abundance (ind m⁻³) at each station in (a) February, (b) April, (c) August, and (d) October 2018.

The Shannon–Wiener species diversity index was in the range of 1.27–3.01 (stations 3 and 16, respectively) in February, 1.52–2.63 (stations 3 and 12, respectively) in April, 2.64–3.36 (stations 5 and 12, respectively) in August, and 2.04–3.25 (stations 1 and 17, respectively) in October (Figure 5).

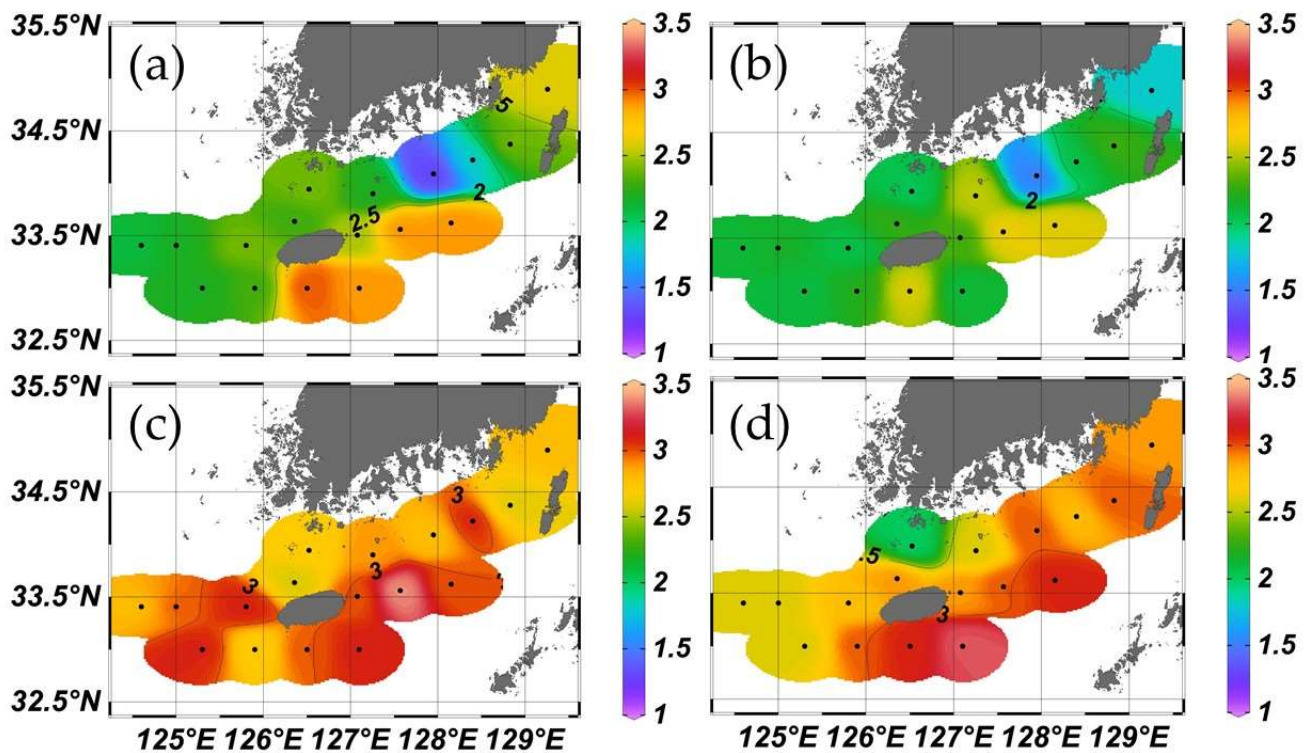


Figure 5. Distribution of the species diversity index based on copepod abundance in (a) February, (b) April, (c) August, and (d) October 2018.

3.3. Cluster Analysis

In February, the stations were divided into west (Group A) and east (Group B) with Jeju Island as the reference point and a similarity index of 50%. The contribution of the grouped stations was highest in the following order in Group A: *Paracalanus parvus* s. 1., *S. longispinosa*, *Calanus sinicus*, *D. affinis*, and *Oithona plumifera*. It was in the following order in Group B: *Paracalanus parvus* s. 1., *Oithona plumifera*, *S. longispinosa*, and *Ctenocalanus vanus* (see Supplementary Material Table S2, Figure 6). In April, the stations were divided into north (Group A) and south (Group B) with Jeju Island as the reference point and a similarity index of 55%. *Paracalanus parvus* s. 1., *Oithona similis*, *D. affinis*, *Calanus sinicus*, and *A. omorii* were important contributors in Group A, whereas *Oithona similis*, *Paracalanus parvus* s. 1., *Oithona longispina*, *Ctenocalanus vanus*, *D. affinis*, *Calanus sinicus*, *Oncaea scottodiarloi*, and *Oithona plumifera* were important contributors in Group B (see Supplementary Material Table S2, Figure 6). In August, the stations were divided into western offshore stations (Group A) and the rest (Group B), using Jeju Island as the reference point (Figure 6). In Group A, *A. pacifica*, *Paracalanus parvus* s. 1., *Calanus sinicus*, *Paracalanus aculeatus*, *Oncaea venella*, *D. affinis*, and *Canthocalanus pauper* were important contributors. By contrast, Group B was divided into Groups B-1 and B-2. *Oncaea venusta*, *Paracalanus parvus* s. 1., *Undinula vulgaris*, *Oncaea venella*, *Oithona atlantica*, *D. affinis*, *Clausocalanus furcatus*, and *Paracalanus aculeatus* made important contributions to Group B-1, whereas in Group B-2, the important contributors were *Paracalanus aculeatus*, *Oncaea venusta*, *Oncaea venella*, *Oithona plumifera*, *Clausocalanus furcatus*, and *Paracalanus parvus* s. 1. (see Supplementary Material Table S2, Figure 6). In October, the stations were divided into two groups (Groups A and B) with a similarity index of approximately 60%. Group A was divided into Groups B-1 and B-2. The highest contributors to the B-1 group were in the following order: *Paracalanus parvus* s. 1., *Paracalanus aculeatus*, *Oncaea venusta*, *D. affinis*, and *A. pacifica*. The highest contributors to Group B-2 were in the following order: *Paracalanus aculeatus*, *Oncaea venusta*, and *Oithona plumifera* (see Supplementary Material Table S2, Figure 6).

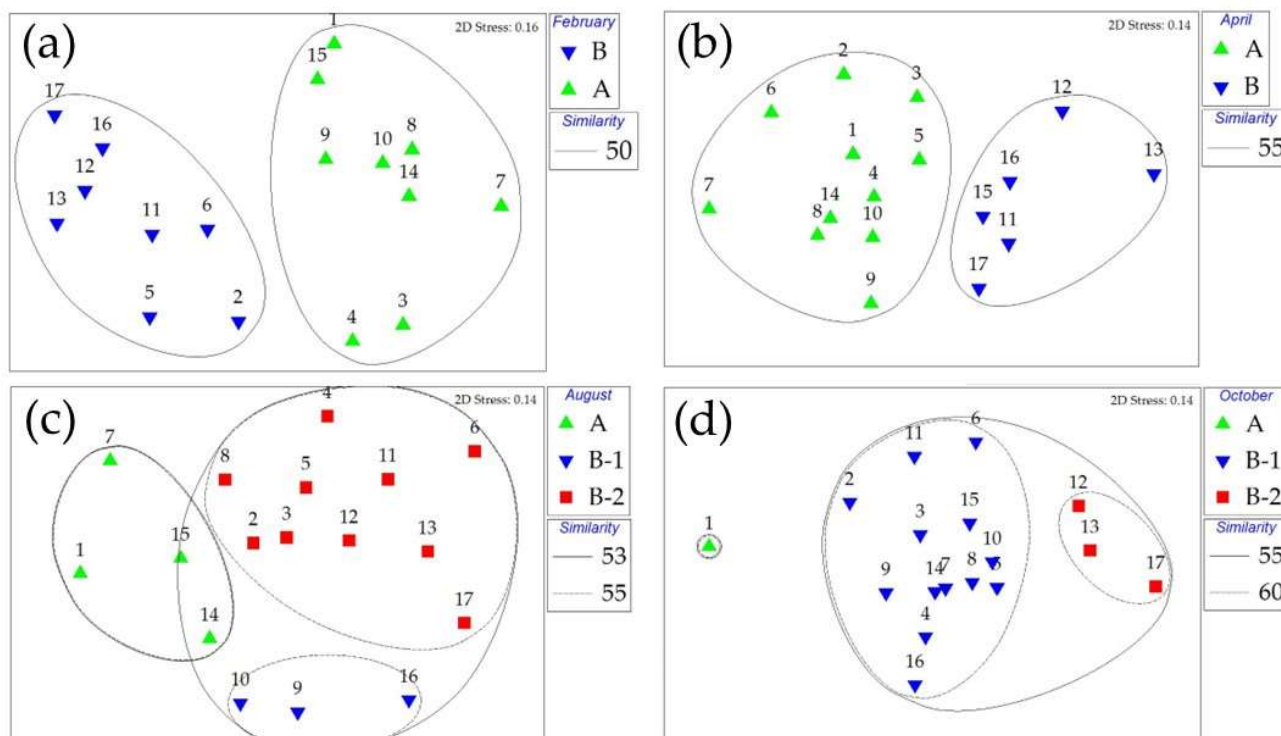


Figure 6. Dendrogram from the cluster analysis based on the Bray–Curtis similarities that were estimated using copepod abundance in the Korea South Sea and a non-metric multidimensional scaling (nMDS) analysis in (a) February, (b) April, (c) August, and (d) October 2018.

3.4. Correlation between the Environmental Factors and Major Copepods

Among the species that played an important role in the grouping of similar community structures in February, *Calanus sinicus*, in Group A, showed a negative correlation with water temperature ($p < 0.01$), and *Oithona plumifera*, in, Group B showed a positive correlation with water temperature and salinity ($p < 0.05$; Table 3, see Supplementary Material Table S3 and Figure S2a). In April, *A. omorii* and *Calanus sinicus*, in Group A, showed a negative correlation with water temperature and salinity, respectively ($p < 0.05$; Table 3, see Supplementary Material Figure S2b). In August, *Oncaea venella*, in Group B-1, showed a positive correlation with salinity and Chl-*a* ($> 20 \mu\text{m}$; $p < 0.01$), whereas *Paracalanus aculeatus* showed a positive correlation with salinity ($p < 0.01$) and Chl-*a* ($> 20 \mu\text{m}$) ($p < 0.05$). *Oncaea venusta*, in Group B-2, showed a positive correlation with the total Chl-*a* ($p < 0.01$; Table 3, see Supplementary Materials Table S3 and Figure S2c). In October, *Oncaea venusta*, in Group B-1, showed a positive correlation with salinity, and *A. pacifica* showed a negative correlation with salinity ($p < 0.05$). Furthermore, *Paracalanus aculeatus*, in Group B-2, showed a positive correlation with Chl-*a* ($>20 \mu\text{m}$; $p < 0.05$; Table 3, see Supplementary Material Table S3).

Table 3. Correlation analysis between species and environmental factors in February (Feb.), April (Apr.), August (Aug.), and October (Oct.) 2018. (** correlation is significant at the 0.01 level, * correlation is significant at the 0.05 level).

Group	Species	T	S	Chlorophyll-a				
				Total	>20 µm	3–20 µm	<3 µm	
Feb.	A	<i>Paracalanus parvulus</i> s. l.	−0.264	0.350	−0.716 *	−0.252	no data	no data
		<i>Scolecithricella longispinosa</i>	0.093	−0.475	−0.310	−0.177	no data	no data
		<i>Calanus sinicus</i>	−0.880 **	−0.207	−0.197	0.212	no data	no data
		<i>Ditrichocorycaeus affinis</i>	0.460	−0.179	0.312	−0.008	no data	no data
		<i>Oithona plumifera</i>	0.435	0.571	−0.056	−0.456	no data	no data
	B	<i>Paracalanus parvulus</i> s. l.	−0.572	−0.234	−0.110	0.050	no data	no data
		<i>Oithona plumifera</i>	0.769 *	0.801 *	0.412	0.409	no data	no data
		<i>Scolecithricella longispinosa</i>	0.589	0.270	0.280	0.229	no data	no data
		<i>Ctenocalanus vanus</i>	−0.197	−0.639	−0.364	−0.550	no data	no data
Apr.	A	<i>Paracalanus parvulus</i> s. l.	−0.163	−0.376	0.094	−0.488	0	0.063
		<i>Oithona similis</i>	−0.479	−0.495	0.226	−0.227	0	0.275
		<i>Ditrichocorycaeus affinis</i>	−0.189	0.139	0.323	0.082	0	0.368
		<i>Calanus sinicus</i>	−0.586	−0.713 *	−0.123	−0.291	0	−0.065
		<i>Acartia omorii</i>	−0.633 *	−0.570	0.104	−0.220	0	0.181
	B	<i>Oithona similis</i>	−0.314	0.108	0.207	−0.081	−0.328	−0.192
		<i>Paracalanus parvulus</i> s. l.	−0.779	0.043	0.419	−0.021	0.137	0.310
		<i>Oithona longispina</i>	−0.016	0.003	−0.101	−0.200	−0.426	−0.407
		<i>Ctenocalanus vanus</i>	0.302	−0.147	−0.749	−0.587	0.313	0.027
		<i>Ditrichocorycaeus affinis</i>	−0.093	−0.356	−0.247	−0.432	0.197	0.053
Aug.	A	<i>Calanus sinicus</i>	0.224	0.139	−0.374	−0.235	0.554	0.403
		<i>Oncaea scottodiarloi</i>	−0.513	−0.470	0.072	−0.392	−0.060	−0.076
		<i>Oithona plumifera</i>	−0.786	−0.107	0.282	−0.131	0.152	0.261
		<i>Acartia pacifica</i>	−0.898	−0.149	0.672	0.712	−0.118	0.219
		<i>Paracalanus parvulus</i> s. l.	−0.657	−0.289	0.574	0.564	−0.437	−0.044
		<i>Paracalanus aculeatus</i>	0.851	0.365	−0.884	−0.235	−0.670	−0.884
		<i>Oncaea venella</i>	−0.204	0.824	−0.501	0.842	−0.540	−0.650
	B−1	<i>Calanus sinicus</i>	0.049	−0.789	0.455	−0.276	−0.491	−0.107
		<i>Ditrichocorycaeus affinis</i>	−0.563	0.339	0.062	0.893	−0.588	−0.411
		<i>Canthocalanus pauper</i>	0.824	0.246	−0.679	−0.639	0.220	−0.154
B−2	<i>Oncaea venusta</i>	−0.207	0.425	0.599	0.087	−0.029	−0.302	
	<i>Paracalanus parvulus</i> s. l.	−0.190	−0.379	−0.135	−0.165	0.023	0.237	
	<i>Undinula vulgaris</i>	0.619	0.388	−0.029	0.430	−0.240	−0.709 *	
	<i>Oncaea venella</i>	0.345	0.780 **	−0.061	0.788 **	0.455	−0.332	
	<i>Oithona atlantica</i>	−0.231	−0.352	0.190	−0.372	−0.503	−0.041	
	<i>Ditrichocorycaeus affinis</i>	0.138	−0.087	−0.530	0.018	−0.420	−0.407	
	<i>Clausocalanus furcatus</i>	0.129	0.351	0.211	−0.082	0.066	−0.173	
B−2	<i>Paracalanus aculeatus</i>	0.076	0.822 **	0.309	0.726 *	0.525	−0.151	
	<i>Paracalanus aculeatus</i>	−0.981	−0.971	0.875	−0.191	0.986	−0.139	
	<i>Oncaea venusta</i>	−0.766	−0.736	1.000 **	0.306	0.785	0.356	
	<i>Oncaea venella</i>	0.529	0.490	−0.951	−0.585	−0.555	−0.627	
	<i>Oithona plumifera</i>	0.813	0.838	−0.246	0.846	−0.795	0.817	
	<i>Clausocalanus furcatus</i>	0.697	0.664	−0.995	−0.400	−0.718	−0.448	
	<i>Paracalanus parvulus</i> s. l.	−0.957	−0.969	0.546	−0.630	0.948	−0.588	
Oct.	B−1	<i>Paracalanus parvulus</i> s. l.	0.067	−0.473	0.006	0.027	0.062	0.414
		<i>Paracalanus aculeatus</i>	0.074	−0.320	−0.089	−0.190	−0.118	0.444
		<i>Oncaea venusta</i>	0.442	0.654 *	0.236	0.207	0.096	−0.012
		<i>Ditrichocorycaeus affinis</i>	−0.176	0.113	−0.301	−0.325	−0.249	0.012
	B−2	<i>Acartia pacifica</i>	−0.004	−0.614 *	−0.266	−0.376	−0.375	0.385
		<i>Paracalanus aculeatus</i>	−0.890	−0.729	0.892	0.999 *	0.139	0.996
		<i>Oncaea venusta</i>	−0.712	−0.489	0.987	0.968	0.431	0.977
	<i>Oithona plumifera</i>	0.687	0.459	−0.992	−0.958	−0.462	−0.970	

T, water temperature; S, salinity.

4. Discussion

Over the past several decades, many studies have revealed that zooplankton species, in particular copepod species, are closely related to large-scale physical processes, such as the transport of water masses by ocean currents [28–36]. In this study, 106 species were found to occur and among them, 85 were warm-water oceanic species. However, there was a seasonal difference: the warm-water oceanic species were most prevalent in summer, and few species appeared in spring (see Supplementary Material Table S1). By contrast, Kang and Hong [17] showed that the number of warm-water oceanic species was the highest in autumn, and they explained that this was because the force of the TWC increases as autumn approaches [37]. For the past three decades, the warm-water oceanic species from Korean waters have been introduced along the TWC, which branches from the KW [11,17,22,38]. Nevertheless, Cho et al. [39] argued that the TAWC may have a greater effect on the study area than the TWC in summer. In this study, warm-water oceanic calanoid copepods (59 species) occurred in the Korea South Sea, including species from the TAWC and KW. Among these species, *A. danae*, *Centropages gracilis*, *Nannocalanus minor*, *Euchaeta media*, *Heterorhabdus subspiniifrons*, *Labidocera acuta*, *Pontellina morii*, *Rhincalanus nasutus*, *S. nicobarica*, and *Temoropia mayumbaensis* occurred in the Taiwanese waters, whereas *Clausocalanus parapergens*, *Haloptilus longicornis*, *Rhincalanus cornutus*, *Pleuromamma piseki*, and *S. longispinosa* appeared in the KW. Although the data need to be supplemented by further extensive surveys in the KW, this occurrence pattern seems to support Cho et al. [39]. Moreover, since the study conducted by Kang and Hong [17], the oceanic warm-water species appear to have continuously increased in Korean waters (see Supplementary Material Table S4), likely due to global warming, which could cause changes in the community structure of the zooplankton in the marine ecosystem.

The cluster analysis indicated that the stations were divided into two or three groups (Figure 6). The contributing species for the grouped stations are shown in Table 3. Among them, in winter, the neritic species, *Paracalanus parvus* s. l., showed a significantly negative relationship with the total Chl-*a* ($p < 0.05$) in Group A, but in the other seasons, it was not significantly related to the other environmental factors. The warm-water oceanic species, *Oithona plumifera*, had a significantly positive relationship with temperature and salinity ($p < 0.05$) in Group B in winter. The neritic species *A. omorii* had a significantly negative relationship with temperature ($p < 0.05$) in Group A in spring. The warm-water oceanic species *Oncaea venella* and *Paracalanus aculeatus* were significantly positively related with salinity and Chl-*a* ($>20 \mu\text{m}$) in Group B in summer. Additionally, the warm-water oceanic species *Oncaea venusta* had a positive relationship with salinity ($p < 0.05$), whereas the neritic species *A. pacifica* had a negative relationship with salinity ($p < 0.05$) in Group B in autumn. Additionally, in the correlation analysis between the environmental factors and dominant copepods, *Oithona plumifera* (February, Group B), *Paracalanus aculeatus* (August, Group B-1), *Oncaea venusta* (October, B Group -1), and *Oncaea venella* (August, Group B-1) showed positive correlations with water temperature or salinity, indicating that these species are possible indicators of the TWC. Many studies [3,6–8,40] suggest that *Clausocalanus furcatus*, *Oithona plumifera*, *Paracalanus aculeatus*, *Oncaea venusta*, *Oncaea venella*, *Oncaea mediterranea*, *Oncaea media*, *Triconia conifera*, *Nannocalanus minor*, *Canthocalanus pauper*, *Scolecithrix danae*, *Temora turbinata*, and *Calocalanus plumulosus* are abundant in the KW, which has a high temperature and high saltwater masses, and their occurrence indicates inflow from the TWC (see Supplementary Material Table S4).

In the present study, as a result of examining the correlation between the dominant species and the phytoplankton, three species, namely *Paracalanus aculeatus*, *Oncaea venusta*, and *Oncaea venella*, showed a positive correlation with >20 -micrometer phytoplankton. It is easy for zooplankton to find and capture large prey [41]. Although analyzing the relationship with phytoplankton according to the size of the zooplankton is ideal, a limitation of the present study is its understanding of the food web from phytoplankton to zooplankton, because size was not measured.

By contrast, the neritic cold-water species, *Calanus sinicus*, was a key species in Group A in summer. *Calanus sinicus* was well distributed in the YSBCW in summer [9,10]. The YSBCW is formed in the winter and remains in the bottom layer, and as the seasons change, and the surface water temperature rises under the influence of the rising temperature of the seasons; consequently, a strong stratification with the bottom water is created, and it flows south to the Korea South Sea in all seasons except winter [42,43]. In April, August, and October, the YSBCW was found in the bottom layers at <50 m in the western sea area (stations 1, 7, 8, 9, 14, and 15) based on Jeju Island. In August and October, it extended to the western area of the study area, and the extension range was the narrowest in April (stations 7 and 14). *Calanus sinicus*, which appeared in the areas where the YSBCW was observed between April and October, had a higher average abundance, including immature individuals, than in other waters: 842 ind m⁻³ in April, 200 ind m⁻³ in August, and 57 ind m⁻³ in October. Furthermore, in April, the high abundance in the western area (station 7) was due to the high abundance of the copepods stage of the *Calanus sinicus*. These results suggest that the southern flow of the YSBCW can affect the copepod community of the Korea South Sea. However, the geographical distribution of *Calanus sinicus* extends southward to northeastern Taiwan in the marginal seas of the northwestern Pacific Ocean [3,33,35,43]. Moreover, *Calanus sinicus* retains its population in cold water at <20 °C in the Yeosu Strait of Gwangyang Bay, located in the central region of the southern Korea South Sea in summer [11]. This indicates that *Calanus sinicus* can have variable sites for its overwintering period [9,10].

The species diversity index could also have responded to the effect of the inclusion of the warm currents. Tseng et al. [5] suggested that when comparing the species diversity indices in seas where various water masses exist, the species diversity index is usually higher in sea areas that are affected by warm currents. In this study, most of the stations that were affected by the TWC showed a high species diversity index, and it seems that the inflow of the oceanic warm currents, such as the TWC, could have affected the species diversity index. In August, the TWC and YSBCW flowed together in the waters near the western part of Jeju Island (stations 8 and 9), indicating that these water masses may have contributed to the increase in the species diversity index. However, the CDW, which is known to affect the Korea South Sea in the summer, was not recorded during the study period. This may be because the inflow of the CDW in 2018 (<45,000 m³ s⁻¹) was significantly lower than in 2016, 2017, 2019, and 2020 (approximately 60,000–80,000 m³ s⁻¹) [<https://www.nifs.go.kr/bbs?id=insmaterial&flag=pre&boardIdx=3861&site=&gubun=A&sc=&sv=&cPage=1&startDate=&endDate=>], accessed on 20 April 2022.

5. Conclusions

There are various water masses or currents in the Korea South Sea, and the spatiotemporal occurrence pattern of the planktonic copepods seems to be affected by the seasonal fluctuations in these water masses. In particular, some of the following are possible indicator species: *Oithona plumifera*, *Oncaea venusta*, and *Paracalanus aculeatus* for the TWC, *Calanus sinicus* for the YSBCW, and *A. pacifica* for coastal waters. Moreover, as global warming intensifies, studies on zooplankton diversity are expected to play an important role in determining the fluctuations in various water masses.

Supplementary Materials: The following supporting information can be downloaded at: <https://www.mdpi.com/article/10.3390/jmse10060754/s1>. Table S1: Abundance of the copepods; Table S2: Similarity-percentages (SIMPER) analysis; Table S3: Canonical correspondence analysis (CCA) table; Table S4: Warm-water species; Figure S1: Distribution of chlorophyll-a concentration; Figure S2: Canonical correspondence analysis (CCA) figure. References [44–47] are cited in Supplementary Materials.

Author Contributions: Conceptualization, S.S.S., S.Y.C., M.H.S., S.J.L., H.Y.S. and S.H.Y.; methodology, S.S.S. and H.Y.S.; software, S.S.S. and S.Y.C.; validation, H.Y.S.; investigation, S.H.Y.; resources, S.H.Y.; data curation, S.S.S., M.H.S., S.J.L. and H.Y.S.; writing—original draft preparation, S.S.S., S.Y.C. and H.Y.S.; writing—review and editing, H.Y.S.; visualization, S.S.S. and S.Y.C.; supervision, S.H.Y.; project administration, H.Y.S.; funding acquisition, H.Y.S. All authors have read and agreed to the published version of the manuscript.

Funding: This research was funded by the National Institute of Fisheries Science (NIFS), Korea, effects of typhoons on the marine ecosystem in Korea, grant number R2022058.

Institutional Review Board Statement: Not applicable.

Data Availability Statement: Not applicable.

Acknowledgments: We thank the anonymous reviewers and the editor, who made constructive and invaluable suggestions and comments.

Conflicts of Interest: The authors declare no conflict of interest.

References

1. Haury, L.R.; Yamazaki, H.; Fey, C.L. Simultaneous measurements of small-scale physical dynamics and zooplankton distributions. *J. Plankton Res.* **1992**, *14*, 513–530. [[CrossRef](#)]
2. Uye, S.; Shimazu, T.; Yamamuro, M.; Ishitobi, Y.; Kamiya, H. Geographical and seasonal variations in mesozooplankton abundance and biomass in relation to environmental parameters in Lake Shinji-Ohashi River-Lake Nakaumi brackish-water system. *J. Mar. Syst.* **2000**, *26*, 193–207. [[CrossRef](#)]
3. Hwang, J.S.; Wong, C.K. The China coastal current as a driving force for transporting *Calanus sinicus* (Copepoda: Calanoida) from its population centers to waters of Taiwan and Hong Kong during the NE monsoon period in winter. *J. Plankton Res.* **2005**, *27*, 205–210. [[CrossRef](#)]
4. Hwang, J.S.; Souissi, S.; Tseng, L.C.; Seuront, L.; Schmitt, F.G.; Fang, L.S.; Peng, S.H.; Wu, C.H.; Hsiao, S.H.; Twan, W.H.; et al. A 5-year study of the influence of the northeast and southwest monsoons on copepod assemblages in the boundary coastal waters between the East China Sea and the Taiwan Strait. *J. Plankton Res.* **2006**, *28*, 943–958. [[CrossRef](#)]
5. Tseng, L.C.; Souissi, S.; Dahms, H.U.; Chen, Q.C.; Hwang, J.S. Copepod communities related to water masses in the southwest East China Sea. *Helgol. Mar. Res.* **2008**, *62*, 153–165. [[CrossRef](#)]
6. Hsieh, C.H.; Chiu, T.S.; Shih, C.T. Copepod diversity and compositions as indicators of intrusion of the Kuroshio branch current into the Northern Taiwan Strait in spring 2000. *Zool. Stud.* **2004**, *43*, 393–403.
7. Liao, C.H.; Chang, W.J.; Lee, M.A.; Lee, K.T. Summer distribution and diversity of copepods in the upwelling waters of the southeastern East China Sea. *Zool. Stud.* **2006**, *45*, 378–394.
8. Lan, Y.C.; Lee, M.A.; Liao, C.H.; Lee, K.T. Copepod community structure of the winter frontal zone induced by the Kuroshio Branch Current and the China Coastal Current in the Taiwan Strait. *J. Mar. Sci. Technol.* **2009**, *17*, 1–6. [[CrossRef](#)]
9. Wang, R.; Zuo, T.; Wang, K. The Yellow Sea cold bottom water—an overwintering site for *Calanus sinicus* (Copepoda, Crustacea). *J. Plankton Res.* **2003**, *25*, 169–183. [[CrossRef](#)]
10. Pu, X.M.; Sun, S.; Yang, B.; Zhang, G.T.; Zhang, F. Life history strategies of *Calanus sinicus* in the southern Yellow Sea in summer. *J. Plankton Res.* **2004**, *26*, 1059–1068. [[CrossRef](#)]
11. Jang, M.C.; Jang, P.G.; Shin, K.S.; Park, D.W.; Jang, M. Seasonal variation of zooplankton community in Gwangyang Bay. *Korean J. Environ. Biol.* **2004**, *22*, 11–29.
12. Moon, S.Y.; Oh, H.J.; Soh, H.Y. Seasonal variation of zooplankton communities in the southern coastal waters of Korea. *Ocean Polar Res.* **2010**, *32*, 411–426. [[CrossRef](#)]
13. Cho, Y.K.; Kim, K. Characteristics and origin of the cold water in the South Sea of Korea in summer. *Korean Soc. Oceanogr.* **1994**, *29*, 414–421.
14. Eisner, L.; Hillgruber, N.; Martinson, E.; Maselko, J. Pelagic fish and zooplankton species assemblages in relation to water mass characteristics in the northern Bering and southeast Chukchi seas. *Polar Biol.* **2013**, *36*, 87–113. [[CrossRef](#)]
15. Park, C.; Lee, C.R.; Kim, J.C. Zooplankton community in the front zone of the East Sea (Sea of Japan), Korea: 2. Relationship between abundance distribution and seawater temperature. *Korean J. Fish. Aquat. Sci.* **1998**, *31*, 749–759.
16. Park, J.S.; Lee, S.S.; Kang, Y.S.; Lee, B.D.; Huh, S.H. The distributions of copepods and chaetognaths in the southern waters of Korea and their relationship to the characteristics of water masses. *Korean J. Fish. Aquat. Sci.* **1990**, *23*, 245–252.
17. Kang, Y.S.; Hong, S.Y. Occurrences of oceanic warm-water calanoid copepods and their relationship to hydrographic conditions in Korean waters. *Bull. Plankton Soc. Jpn. Hiroshima* **1995**, *42*, 29–41.
18. Lee, C.R.; Lee, P.G.; Park, C. Seasonal and vertical distribution of planktonic copepods in the Korea Strait. *Korean J. Fish. Aquat. Sci.* **1999**, *32*, 525–533.

19. Choi, S.Y. Spatial and Temporal Distribution of Acartia (Crustacea, Copepoda, Calanoida) Species in the Southern Coastal Waters of Korea and the Physio-Ecological Characteristics of Acartia erythraea. Ph.D. Thesis, Chonnam National University, Yeosu, Korea, February 2020.
20. Kondo, M. Oceanographic investigations of fishing grounds in the East China Sea and the Yellow Sea-I. Characteristics of the mean temperature and salinity distributions measured at 50 m and near the bottom. *Bull. Seikai Reg. Fish. Res. Lab.* **1985**, *62*, 19–66.
21. Lie, H.J.; Cho, C.H. Seasonal circulation patterns of the Yellow and East China Seas derived from satellite-tracked drifter trajectories and hydrographic observations. *Prog. Oceanogr.* **2016**, *146*, 121–141. [[CrossRef](#)]
22. Park, J.S.; Lee, S.S.; Kang, Y.S.; Huh, S.H. Distribution of indicator species of copepods and chaetognaths in the middle East Sea of Korea and their relationships to the characteristics of water masses. *Korean J. Fish. Aquat. Sci.* **1991**, *24*, 203–212.
23. Vohra, D.F. *Determination of Photosynthetic Pigments in SeaWater. Monographs on Oceanographic Methodology*; UNESCO, Ed.; UNESCO: Paris, France, 1996; pp. 10–18.
24. Seung, Y.H. Water masses and circulations around Korean Peninsula. *J. Korean Soc. Oceanogr.* **1992**, *27*, 324–331.
25. Jang, S.T.; Lee, J.H.; Kim, C.H.; Jang, C.J.; Jang, Y.S. Movement of cold water mass in the northern East China Sea in summer. *J. Korea Soc. Oceanogr.* **2011**, *16*, 1–13.
26. Gong, G.C.; Chen, Y.L.L.; Liu, K.K. Chemical hydrography and chlorophyll-a distribution in the East China Sea in summer: Implications in nutrient dynamics. *Cont. Shelf Res.* **1996**, *16*, 1561–1590. [[CrossRef](#)]
27. Clarke, K.R.; Gorley, R.N. *Primer v6: User Manual/Tutorial*; PRIMER-E: Plymouth, UK, 2006; p. 866.
28. Ter Braak, C.J.F.; Milauer, P. *CANOCO Reference Manual and CanoDraw for Windows User's Guide: Software for Canonical Community Ordination (Version 4.5)*; Microcomputer Power: Ithaca, NY, USA, 2002.
29. Haury, L.R.; Pieper, R.E. *Zooplankton: Scales of biological and physical events. Marine Organisms as Indicators*; Springer: New York, NY, USA, 1988; pp. 35–72.
30. Yuhui, L.; Nakamura, Y. Distribution of planktonic copepods in the Kuroshio area of the East China Sea to the southwest of Kyushu in Japan. *Acta Oceanol. Sin.* **1993**, *3*, 445–456.
31. Beaugrand, G.; Reid, P.C.; Ibanez, F.; Lindley, J.A.; Edwards, M. Reorganization of North Atlantic marine copepod biodiversity and climate. *Science* **2002**, *296*, 1692–1694. [[CrossRef](#)] [[PubMed](#)]
32. Peterson, W.T.; Keister, J.E. Interannual variability in copepod community composition at a coastal station in the northern California Current: A multivariate approach. *Deep Sea Res. Part II Top. Stud. Oceanogr.* **2003**, *50*, 2499–2517. [[CrossRef](#)]
33. Dur, G.; Hwang, J.S.; Souissi, S.; Tseng, L.C.; Wu, C.H.; Hsiao, S.H.; Chen, Q.C. An overview of the influence of hydrodynamics on the spatial and temporal patterns of calanoid copepod communities around Taiwan. *J. Plankton Res.* **2007**, *29*, 97–116. [[CrossRef](#)]
34. Hwang, J.S.; Dahms, H.U.; Tseng, L.C.; Chen, Q.C. Intrusions of the Kuroshio Current in the northern South China Sea affect copepod assemblages of the Luzon Strait. *J. Exp. Mar. Biol. Ecol.* **2007**, *352*, 12–27. [[CrossRef](#)]
35. Hsiao, S.H.; Kâ, S.; Fang, T.H.; Hwang, J.S. Zooplankton assemblages as indicators of seasonal changes in water masses in the boundary waters between the East China Sea and the Taiwan Strait. *Hydrobiologia* **2011**, *666*, 317–330. [[CrossRef](#)]
36. Sogawa, S.; Kidachi, T.; Nagayama, M.; Ichikawa, T.; Hidaka, K.; Ono, T.; Shimizu, Y. Short-term variation in copepod community and physical environment in the waters adjacent to the Kuroshio Current. *J. Oceanogr.* **2017**, *73*, 603–622. [[CrossRef](#)]
37. Teague, W.J.; Jacobs, G.A.; Perkins, H.T.; Book, J.W.; Chang, K.I.; Suk, M.S. Low-frequency current observation in the Korea/Tsushima Strait. *J. Phys. Oceanogr.* **2002**, *32*, 1621–1641. [[CrossRef](#)]
38. Kim, W.S.; Yoo, J.M.; Myung, C.S. A review on the copepods in the South Sea of Korea. *Korean J. Fish. Aquat. Sci.* **1993**, *26*, 266–278.
39. Cho, Y.K.; Seo, G.H.; Choi, B.J.; Kim, S.; Kim, Y.G.; Youn, Y.H.; Dever, E.P. Connectivity among straits of the northwest Pacific marginal seas. *J. Geophys. Res. Ocean.* **2009**, *114*, C06018. [[CrossRef](#)]
40. Lee, C.Y.; Liu, D.C.; Su, W.C. Seasonal and spatial variations in the planktonic copepod community of Ilan Bay and adjacent Kuroshio waters off northeastern Taiwan. *Zool. Stud.* **2009**, *48*, 151–161.
41. Stoecker, D.K.; Eglhoff, D.A. Predation by Acartia tonsa Dana on planktonic ciliates and rotifers. *J. Exp. Mar. Biol. Ecol.* **1987**, *110*, 53–68. [[CrossRef](#)]
42. Yun, Y.H.; Park, Y.H.; Bong, J.H. Enlightenment of the characteristics of the Yellow Sea bottom cold water and its southward extension. *J. Korean Earth Sci. Soc.* **1991**, *12*, 25.
43. Choi, Y.C. The Characteristics of Yellow Sea Bottom Cold Water in September, 2006. *J. Fish. Mar. Sci. Educ.* **2011**, *23*, 425–432.
44. Nakata, K.; Itoh, H.; Ichikawa, T.; Sasaki, K. Seasonal changes in the reproduction of three oncaeid copepods in the surface layer of the Kuroshio Extension. *Fish. Oceanogr.* **2004**, *13*, 21–33. [[CrossRef](#)]
45. Ka, S.; Hwang, J.S. Mesozooplankton distribution and composition on the northeastern coast of Taiwan during autumn: Effects of the Kuroshio Current and hydrothermal vents. *Zool. Stud.* **2011**, *50*, 155–163.
46. Tseng, L.C.; Hung, J.J.; Chen, Q.C.; Hwang, J.S. Seasonality of the copepod assemblages associated with interplay waters off northeastern Taiwan. *Helgol. Mar. Res.* **2013**, *67*, 507–520. [[CrossRef](#)]
47. Miyamoto, H.; Itoh, H.; Okazaki, Y. Temporal and spatial changes in the copepod community during the 1974–1998 spring seasons in the Kuroshio region; a time period of profound changes in pelagic fish populations. *Deep Sea Res. Part I Oceanogr. Res. Pap.* **2017**, *128*, 131–140. [[CrossRef](#)]